

Localization simulation of graphene photonic crystal doped tin oxide

Zhenghua Yao

School of Physics, Hubei University, Wuhan, 430062, China

Abstract: Photonic crystal is an optical microstructure whose dielectric constant is periodically modulated by spatial position. The structure of photonic crystal can be divided into one-dimensional, two-dimensional and three-dimensional, and two-dimensional has become a research hotspot. For the photonic crystal doped with tin oxide in two-dimensional hexagonal graphene, this paper uses COMSOL software to solve the energy band of the lattice on the basis of triangular cell, and obtains the electric field height image and energy band structure diagram under TM and TE modes. The localization of the electric field and the band gap structure of the two modes in a certain frequency range are analyzed. It provides a simulation method and theoretical basis for the application of this material.

Keywords: photonic crystal, band gap, localization

1. Introduction

In 1987, S. John first proposed photonic crystal, which is a microstructure composed of dielectrics with different refractive indices arranged periodically. It has important characteristics of photonic localization and photonic band gap [1]. According to these characteristics, photonic crystals can be used to manufacture high-performance devices such as efficient semiconductor lasers, optical filters, waveguides, and optical amplifiers.

YUAN et al proposed the method of DtN mapping to calculate the band gap structure of two-dimensional photonic crystals with positive and triangular arrangement [2]. Zhang et al proposed a new type of two-dimensional lattice photonic crystal with different windmill shape defects, and studied the influence of the translation and rotation of the defect structure of different windmill models on the transverse magnetic field band gap, further reducing the defect symmetry of the photonic crystal [3]. Based on the traditional plane wave expansion method, Gharaati Abdolrasoul et al proposed a general method for calculating the Faraday rotation and transmission spectra of two-dimensional magneto-optical photonic crystals based on the plane wave expansion method [4]. Dena M. El-Amassi et al assumed that one of the layers constituting the ternary photonic crystal is a left-handed material with both negative permittivity and permeability. It is found that with the increase of the thickness of the LHM layer, the band gap of the one-dimensional ternary photonic crystal will increase significantly [5]. You-Ming Liu et al used the transfer matrix method to study the band gap structure of photonic crystals of magnetized ferrite, and found that the band gap width increases first and then decreases with the increase of disorder effect [6]. Upadhyay A, Taya S. studied a kind of photonic crystal with (AB)NA structure, and studied the change of the band gap width of the photonic crystal with different parameters of the superconducting layer [7]. Fan Y realizes the rapid reconstruction of plasma photonic crystals by using the self-organization of filaments in dielectric barrier discharge. It is found that when the structure of plasma photonic crystals changes, the position and size of band gap will change significantly [8]. Rahmani Z, Rezaee N et al., studied the reflection and absorption of electromagnetic waves in one-dimensional ternary plasmonic photonic crystals by transfer matrix method [9]. Pourmahmoud V, Rezaei B et al. used the Kronig-Penney method to study the electric polarization and magnetic polarization photonic band gap characteristics of one-dimensional photonic crystals composed of dielectric layers and multilayer dielectric graphene layers in the terahertz frequency region [10]. Chen Y H et al studied the phenomenon and reason of the photonic band gap shift of three-dimensional photonic crystals in an open environment of 10 °C and 20 °C [11]. Based on the 2×2 transfer matrix method, Saeidi et al used MATLAB software to theoretically calculate the photonic band gap characteristics and electric field distribution of one-dimensional multi-period photonic crystals [12]. Dga B et al introduced a new type of windmill-like defect, and used the plane wave expansion method to numerically analyze the photonic band gap and defect mode [13].

The two-dimensional hexagonal graphene doped tin oxide photonic crystal was simulated by COMSOL, and the electric field height image and energy band structure diagram in two modes were obtained. The localization of the electric field and the band gap structure of the two modes in a certain frequency range were analyzed.

2. Principle

The propagation of electromagnetic waves in photonic crystals can be described by Maxwell equations[14]:

$$\begin{cases} \nabla \cdot \mathbf{D} = \rho \\ \nabla \cdot \mathbf{B} = 0 \\ \nabla \times \mathbf{E} + \frac{\partial \mathbf{B}}{\partial t} = -\mathbf{J} \\ \nabla \times \mathbf{H} - \frac{\partial \mathbf{D}}{\partial t} = \mathbf{J} \end{cases} \quad (1)$$

E and B are macroscopic electromagnetic and magnetic induction fields, D is the electric displacement vector, and H is the magnetic field. ρ and J are free charge density and current density.

Because photonic crystals are non-magnetic materials, there are

$$\mathbf{B} = \mu_0 \mu(\mathbf{r}) \mathbf{H} \quad (2)$$

$$\mathbf{D} = \epsilon_0 \epsilon(\mathbf{r}) \mathbf{E} \quad (3)$$

Where μ_0 and ϵ_0 are the relative permeability and relative dielectric constant in vacuum, $\mu(\mathbf{r})$ and $\epsilon(\mathbf{r})$ are the relative permeability and relative dielectric constant. The relative permeability of most materials is $\mu(\mathbf{r}) = 1$. Here $\epsilon(\mathbf{r})$ is the position periodic function.

Therefore, the following wave equation can be derived from the Maxwell equations [15]

$$\frac{1}{c^2} \frac{\partial^2 \mathbf{D}}{\partial t^2} + \nabla \cdot \left(\frac{1}{\epsilon(\mathbf{r})} \nabla \times \mathbf{D} \right) = 0 \quad (4)$$

Where c is the speed of light, $c = (\mu_0 \epsilon_0)^{-1/2}$.

Equation (4) is transformed into the steady state equation of electric displacement vector D

$$-\nabla^2 \mathbf{D} - \nabla \times \nabla [\chi(\mathbf{r}) \mathbf{D}] = \frac{\omega^2}{c^2} \mathbf{D} \quad (5)$$

Where ω is the frequency, $\chi(\mathbf{r}) = 1 - 1/\epsilon(\mathbf{r})$.

Considering only the propagation of electromagnetic wave in z direction, (2) can be simplified as

$$\frac{d^2}{dz^2} E(z) + \frac{\omega^2}{c^2} \epsilon(z) E(z) = 0 \quad (6)$$

A unit cell structure of the photonic crystal is shown in Figure 1, which is a layered periodic medium containing two thin layers of alternating thickness d_1 and d_2 , respectively. The dielectric constants of the thin layers are ϵ_1 and ϵ_2 , and the lattice spacing is a .

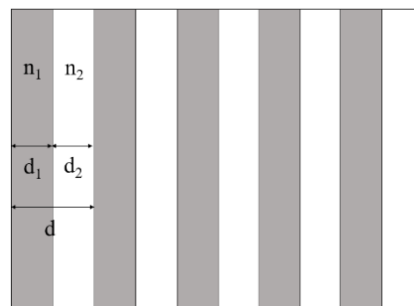


Figure 1: Photonic crystal unit cell periodic structure

The periodicity of the dielectric constant can be written as

$$\epsilon(z + a) = \epsilon(z) \quad (7)$$

Equation (7) makes the solution of Equation (6) have the form of Bloch wave, namely

$$E(z + a) = e^{ikd}E(z) \tag{8}$$

From this, we can further write the solution of the first and second thin layers of the l th unit cell and the first thin layer of the $l + 1$ th unit cell:

$$E_l^{(1)}(z) = A_l e^{iq_1 z} + B_l e^{-iq_1 z} \tag{9}$$

$$E_l^{(2)}(z) = C_l e^{iq_1 z} + D_l e^{-iq_1 z} \tag{10}$$

$$E_{l+1}^{(1)}(z) = A_{l+1} e^{iq_1 z} + B_{l+1} e^{-iq_1 z} \tag{11}$$

Define $q_1 = \varepsilon_1^{1/2} \omega / c = n_1 \omega / c$, $q_2 = \varepsilon_2^{1/2} \omega / c = n_2 \omega / c$, n_1 and n_2 are refractive index. A_l, B_l, C_l and D_l are the amplitudes of the electric field. Taking the left side of each thin layer as the origin of coordinates, then according to the continuity conditions of E and dE / dz on the boundary, we can obtain

$$\begin{pmatrix} A_{l+1} \\ B_{l+1} \end{pmatrix} = T \begin{pmatrix} A_l \\ B_l \end{pmatrix} \tag{12}$$

where T is a 2×2 unimodular transfer matrix, and its matrix element is

$$T_{11} = e^{iq_1 d_1} \left[\cos(q_2 d_2) + \frac{i}{2} \left(\frac{n_1}{n_2} + \frac{n_2}{n_1} \right) \sin(q_2 d_2) \right] \tag{13}$$

$$T_{12} = e^{iq_1 d_1} \frac{i}{2} \left(\frac{n_1}{n_2} - \frac{n_2}{n_1} \right) \sin(q_2 d_2) \tag{14}$$

$$\begin{cases} T_{21} = T_{12}^* \\ T_{22} = T_{11}^* \end{cases} \tag{15}$$

Then Equation (8) is equivalent to

$$\begin{pmatrix} A_{l+1} \\ B_{l+1} \end{pmatrix} = e^{ika} \begin{pmatrix} A_l \\ B_l \end{pmatrix} \tag{16}$$

Substituting Equation (16) into Equation (12), we can get

$$(T - e^{ikd}I) \begin{pmatrix} A_l \\ B_l \end{pmatrix} = 0 \tag{17}$$

where k is the wave vector.

If we consider the inverse process of A_l, B_l to A_{l-1}, B_{l-1} , we can obtain

$$(T^{-1} - e^{ikd}I) \begin{pmatrix} A_l \\ B_l \end{pmatrix} = 0 \tag{18}$$

Combining Equations (17) and (18), we can get

$$\cos kd = \frac{1}{2}(T + T^{-1}) = \frac{1}{2}T_1 T \tag{19}$$

Finally, a transcendental equation is obtained:

$$\cos k(d_1 + d_2) = \cos \frac{n_1 \omega d_1}{c} \cos \frac{n_2 \omega d_2}{c} - \frac{1}{2} \left(\frac{n_1}{n_2} + \frac{n_2}{n_1} \right) \sin \frac{n_1 \omega d_1}{c} \sin \frac{n_2 \omega d_2}{c} \tag{20}$$

The dispersion relation of electromagnetic wave propagation in photonic crystal in one-dimensional periodic structure can be determined by (20).

The eigensolutions and dispersion relations of the one-dimensional complete monatomic chain system are:

$$u_n = A e^{i[qnd - \omega(q)t]}, q \in 1BZ \tag{21}$$

$$\omega(q) = \omega_m \left| \sin \frac{1}{2} qd \right|, \omega_m = 2 \sqrt{\frac{\beta}{M}} \tag{22}$$

Where ω_m is the maximum frequency, $\beta = 1 / k_B T$, k_B is Boltzmann constant, M is atomic mass, $1BZ$ is the first Brillouin zone.

There is no eigensolution of $\omega > \omega_m$ in the complete crystal chain. Suppose there is a solution

$\text{Re}(q) > 0$, then $\sin(1/2qd) = \omega / \omega_m > 1$, so q must be complex and can be written

$$\begin{cases} q = q_1 + iq_2 \\ q_2 \neq 0 \end{cases} \quad (23)$$

Thus can be obtained

$$\frac{\omega}{\omega_m} = \sin \frac{1}{2} q_1 d \operatorname{arcosh} \frac{1}{2} q_2 d + i \cos \frac{1}{2} q_1 d \sinh \frac{1}{2} q_2 d \quad (24)$$

If ω and ω_m are real numbers, $q_2 \neq 0$, then there must be

$$\frac{1}{2} q_1 d = \left(h \pm \frac{1}{2} \right) \pi \quad (25)$$

Solved

$$q_1 = \left(h \pm \frac{1}{2} \right) \frac{2\pi}{d} = K_h \pm \frac{\pi}{d} \quad (26)$$

Since $q_1 \in 1BZ$, there is $q_1 = \pi / d$. Substitute q_1 into Equation (13) to obtain $q_2 = 2 / a * \operatorname{arcosh} (\omega / \omega_m)$. Thus we can be obtained

$$q = \frac{\pi}{d} + i \frac{2}{a} \operatorname{arcosh} \frac{\omega}{\omega_m} \quad (27)$$

Substituting Equation (27) into Equation (21), we can get

$$u_n = A(-1)^n e^{-n\alpha} e^{-i\omega t} \quad (28)$$

where $\alpha = 2 \operatorname{arcosh} (\omega / \omega_m)$. The negative sign of the exponential factor $e^{-n\alpha}$ in Equation (15) corresponds to the exponential attenuation of the amplitude in the propagation direction of the wave vector. Similarly, similar models with $\operatorname{Re}(q) < 0$ can get the same results. Therefore, if there is a vibration mode of $\omega > \omega_m$ in the atomic chain, this mode must be localized near an atom in the atomic chain, which can be seen as the atom is different from other atoms or the atom is missing, as shown in Figure 2, the n th atom is different from other atoms, then the vibration mode edge of $\omega > \omega_m$ is localized near n atoms, as shown in Figure 3. This vibration mode is called local mode [16].

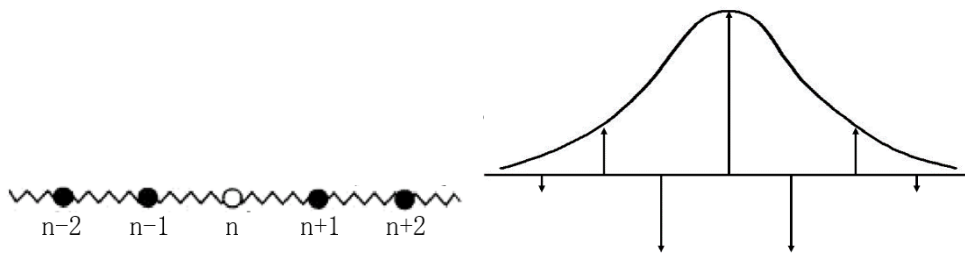


Figure 2: One-dimensional atomic chain with a single atom

Figure 3: Local vibration

3. Numerical calculation and result analysis

The energy band of two-dimensional hexagonal graphene photonic crystal after doping is analyzed, and the doping material is tin oxide. The basic parameters of the two-dimensional hexagonal graphene doped photonic crystal are: the relative dielectric constant of the background medium graphene is $\epsilon_c = 4.5$, and the tin oxide column is $\epsilon_a = 8$. The two-dimensional hexagonal graphene doped photonic crystal structure diagram is shown in Figure 4. The radius of the tin oxide pillar is $r = 0.05a$, $a = 1\text{nm}$, a is the lattice constant. Filling ratio is 0.009068. The first Brillouin zone of the triangular lattice is shown in Figure.5, and the scanning direction of COMSOL is $\Gamma \rightarrow M \rightarrow K$.

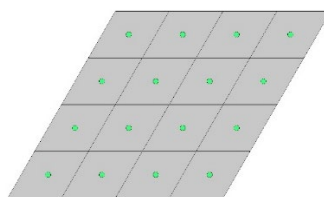


Figure 4: Two-dimensional hexagonal

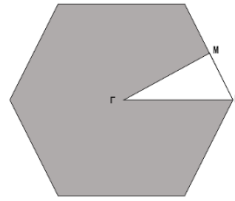


Figure 5: The first Brillouin zone of triangular lattice graphene doped photonic crystal structure

The electric field height of TM mode and TE mode of two-dimensional hexagonal graphene doped photonic crystal obtained by COMSOL simulation is shown in Figure 6 and Figure 7. It can be seen that the electric field has obvious local vibration near the tin oxide.

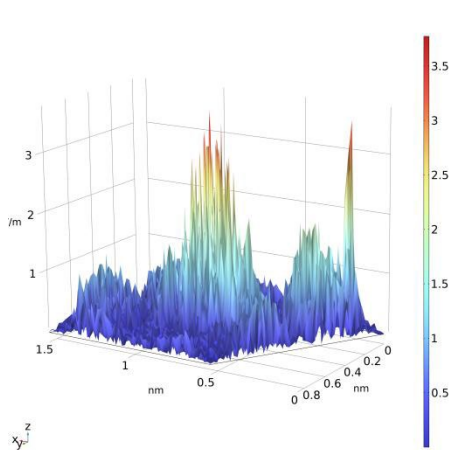


Figure 6: TM mode electric field height

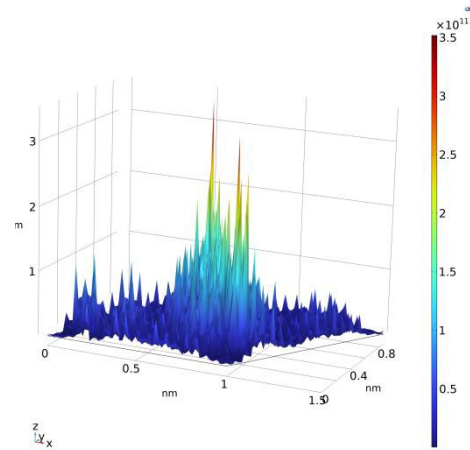


Figure 7: TM mode electric field height

The band structure of TM mode in two-dimensional hexagonal graphene doped photonic crystal is shown in figure 8. It can be seen from Figure 8 that the TM mode of the structure has two band gaps in the range of $f = 15.222 \sim 15.258\omega$. The ranges are $f_1 = 15.232 \sim 15.236\omega$, $f_2 = 15.249 \sim 15.252\omega$, and the band gap widths are $\Delta\omega_1 = 0.04\omega$ and $\Delta\omega_2 = 0.03\omega$, respectively. The band gap diagram of the TE mode is shown in Figure 9. It can be seen that the TE mode of the structure has two band gaps in the range of $f = 16.469 \sim 16.490\omega$, ranging from $f_1 = 16.469 \sim 16.472\omega$ and $f_2 = 16.474 \sim 16.482\omega$, respectively. The band gap widths are $\Delta\omega_1 = 0.03\omega$ and $\Delta\omega_2 = 0.08\omega$, respectively.

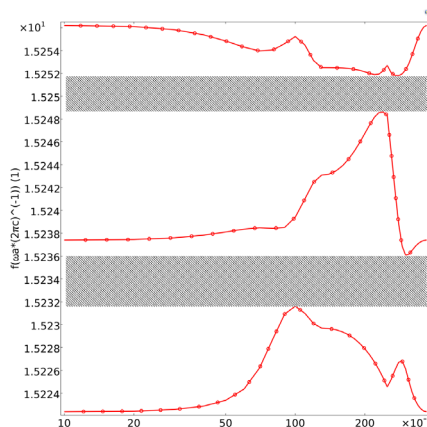


Figure 8: TM mode band structure

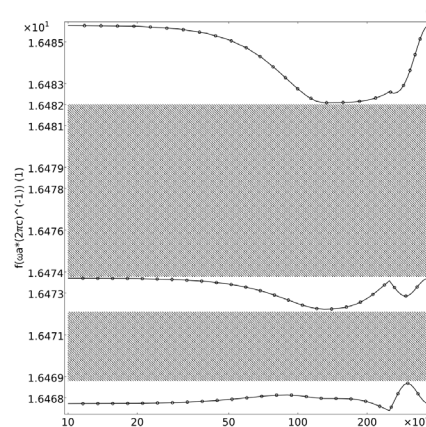


Figure 9: TE mode band structure

4. Conclusions

In this paper, COMSOL software is used to study the band structure and localization of the crystal of two-dimensional hexagonal graphene doped with photons after partial tin oxide. The results show that the material has different degrees of localization near the tin oxide in both TE and TM modes. In the range of $f = 15.222 \sim 15.258\omega$, the TM mode has two band gaps, and the band gap widths are $\Delta\omega_1 = 0.04\omega$ and $\Delta\omega_2 = 0.03\omega$. In the range of $f = 16.469 \sim 16.490\omega$, TE mode has two band gaps. The band

gap widths are $\Delta\omega_1 = 0.03\omega$ and $\Delta\omega_2 = 0.08\omega$, respectively. Through the study of the energy band and local mode of the material, this paper can provide simulation method and theoretical basis for the application of this material.

References

- [1] Joannopoulos J D, Johnson S G, Winn J N. *Photonic crystals: molding the flow of light*[M]. Princeton University Press, 1995:2-3.
- [2] Yuan J, Lu Y Y. Computing photonic band structures by Dirichlet-to-Neumann maps:the triangular lattice [J]. *Optics Communications*, 2007 , 273(1):114-120
- [3] Liqiang Zhang, Chenxi Zhu, Sicheng Yu, Zhuoran Zhou, Daohan Ge. Band gap of silicon photonic crystal with square-lattice and windmill-shaped defects [J]. *Results in Physics*, 2021, 31:15054.
- [4] Gharaati A, Tolgari N A. A general method for calculation of Faraday rotation and transmittance in two-dimensional magneto-optic photonic crystals by solving vector-Helmholtz equation in anisotropic media [J]. *Physica Scripta*, 2021, 96(12): 125517.
- [5] El-Amassi D M, Taya S A, Ramanujam N R, et al. Extension of energy band gap in ternary photonic crystal using left-handed materials [J]. *Superlattices & Microstructures*, 2018, 120: Pages 353-362.
- [6] Youming Liu, Baofei Wan, Sisi Rao, Dan Zhang, Haifeng Zhang, Nonreciprocal omnidirectional band gap of one-dimensional magnetized ferrite photonic crystals with disorder [J]. *Physica B: Condensed Matter*, 2022, 645.
- [7] Upadhyay A, Taya S. Properties of band gap for p polarized wave propagation in a binary superconductor dielectric photonic crystal [J]. *Optik*, 2021, 243: 167505.
- [8] Fan Y. Reconfigurable plasma photonic crystals from triangular lattice to square lattice in dielectric barrier discharge [J]. *Physics Letters, A*, 2021, 396(1): 127223.
- [9] Rahmani Z, Rezaee N. The reflection and absorption characteristics of one-dimensional ternary plasma photonic crystals irradiated by TE and TM waves [J]. *Optik*, 2019, 184:134-141.
- [10] Pourmahmoud V, Rezaei B. Manipulation of Bragg and graphene photonic band gaps in one-dimensional photonic crystal containing grapheme [J]. *Optik - International Journal for Light and Electron Optics*, 2019, 185:875-880.
- [11] Chen Y H, Lu Y J, Chang J Y, et al. Impacts of both temperature and condensation on the band gap of photonic crystals around the freezing point[J]. *Optical Materials*, 2021, 121:111596.
- [12] Saeidi F S, Moradi M. A new route to designing a one-dimensional multiperiodic photonic crystal with adjustable photonic band gap and enhanced electric field localization [J]. *Optics Communications*, 2021, 493(5):126999.
- [13] Dga B, Jpl C, Chao M B, et al. Effect of windmill-like-shaped defect on TM photonic band gaps of two-dimensional square-lattice photonic crystals - ScienceDirect[J]. *Results in Physics*, 2020, 16: 102879.
- [14] Babaahmadi V, Montazer M. Synthesis and daylight photocatalytic properties of graphene/self-doped tin oxide/silver ternary nanocomposite on fabric surface[J]. *Journal of Photochemistry and Photobiology A: Chemistry*, 2022, 422:113561-.DOI:10.1016/j.jphotochem.2021.113561.
- [15] Sani M, Farzad M H. Anderson localization of surface plasmons in monolayer graphene[J].*Physical review*, 2018, 97(8):085406.1-085406.5.
- [16] Wang K, Ke X, Wang W, et al. The Impacts of Fluorine-Doped Tin Oxide Photonic Crystals on a Cadmium Sulfide-Based Photoelectrode for Improved Solar Energy Conversion under Lower Incidence[J]. *Catalysts*, 2020.DOI:10.3390/catal10111252.